

# Magnetometric Studies of Catalyst Refuses in Nanocarbon Materials

Irina V. Ovsienko · Lyudmila Yu. Matzuy · Nykolai I. Zakharenko ·  
Nykolai G. Babich · Tetyana A. Len · Yuriy I. Prylutsyy · David Hui ·  
Yuri M. Strzhemechny · Peter C. Eklund

Received: 19 October 2007 / Accepted: 15 December 2007 / Published online: 8 January 2008  
© to the authors 2008

**Abstract** It is shown that magnetometry can be employed as an effective tool to control the content of a ferromagnetic constituent in nanocarbon materials. We propose a thermochemical treatment protocol to achieve extensive cleaning of the source nanocarbon materials from ferromagnetic refuses.

**Keywords** Nanocarbon material · Magnetometry · Carbon nanotubes · Catalyst refuse · Magnetic susceptibility · Thermochemical treatment

## Introduction

There is a number of common procedures to fabricate carbon nanotubes (CNT) by, e.g. thermal sputtering of

graphite in an electric arc, laser evaporation, etc. [1–8]. For any of them, the synthesized substance is a nanocarbon material (NCM) containing not only single-wall and multi-wall CNT, but also amorphous carbon, graphite nanoparticles, and catalyst refuses. Transition metals are commonly used as catalysts for the CNT synthesis. Their contents depend on the synthesis procedure [9–11]. To obtain CNT of the highest possible purity it is therefore vital to understand and control the routes of their rectification. At the same time, it is necessary to control the composition of the synthesized material. For instance, a fast method for quantitative analysis of the amorphous component is based on Raman scattering as described in Refs. [12–15]. The presence of the metallic component is

---

I. V. Ovsienko · L. Yu. Matzuy · N. I. Zakharenko ·  
N. G. Babich · T. A. Len  
Department of Physics, Kyiv National Shevchenko University,  
Volodymyrska Str., 64, 03310 Kyiv, Ukraine

I. V. Ovsienko  
e-mail: ovsienko@mail.univ.kiev.ua

L. Yu. Matzuy  
e-mail: matzui@univ.kiev.ua

N. I. Zakharenko  
e-mail: zakharenko@univ.kiev.ua

N. G. Babich  
e-mail: babich@univ.kiev.ua

T. A. Len  
e-mail: intercalant@mail.univ.kiev.ua

Y. I. Prylutsyy  
Department of Biophysics, Kyiv National Shevchenko  
University, Volodymyrska Str., 64, 03310 Kyiv, Ukraine  
e-mail: prylut@biocc.univ.kiev.ua

D. Hui  
Department of Mechanical Engineering,  
University of New Orleans, New Orleans,  
LA 70148, USA  
e-mail: DHui@uno.edu

Y. M. Strzhemechny (✉)  
Department of Physics and Astronomy,  
Texas Christian University, TCU Box 298840,  
Fort Worth, TX 76129, USA  
e-mail: Y.Strzhemechny@tcu.edu

P. C. Eklund  
Department of Physics, The Pennsylvania State University,  
104 Davey Laboratory, University Park,  
PA 16802-6300, USA  
e-mail: pce3@psu.edu

commonly detected by the X-ray and electron diffraction, although they have low efficiency at low contents and high dispersity of the metallic constituent.

In this article, we report on the possibility of using thermomagnetic measurements to control the presence of metal catalyst residues in the NCM. The suggested method is quite convenient since the allotropic forms of carbon are known to be diamagnetic whereas presence of even low quantities of metal particles promotes the onset of ferromagnetic or paramagnetic behavior of NCM.

## Experimental

The NCM studied here were produced by a low-temperature conversion of a carbon monoxide in a catalytic process through the Bell–Boudoir reaction:  $2\text{CO} = \text{CO}_2 + \text{C}$  [16]. CO mixture with hydrogen has been flowed over a copper substrate with metal catalyst oxides were placed on it [16]. These oxides were partially reduced to a pure metal upon the synthesis process. Three types of catalysts (nickel, iron, and cobalt oxides) have been used for the synthesis of the studied NCM. According to Ref. [17], the as-prepared NCM specimens contain multi-walled CNT, particles of amorphous carbon and particles of the catalyst (specimen #1: nickel nanoparticles, specimen #2:  $\text{Fe}_3\text{O}_4$  nanoparticles, specimen #3: cobalt nanoparticles). Moreover, the structure, the morphology, and the phase composition of the synthesized NCM are determined by the type of the catalyst. For the removal of the metal-catalyst particles, the source material was soaked in strong acid solutions ( $\text{HNO}_3$ ,  $\text{HCl}$ ) [18]. For the removal of the disordered carbon phase particles, the source material was annealed in air or in oxygen atmosphere in a temperature range of 773–873 K. In this range the disordered amorphous carbon phase is burning out whereas the CNT are stable up to 1,173–1,273 K.

Thermochemical treatment of as-prepared NCM involved the following stages: (1) annealing at 823 K for 30 min in air (the SSHOL-1300 laboratory furnace, provided temperature stability with a  $\pm 10^\circ\text{C}$  accuracy) (specimens #1-T, #2-T, #3-T); (2) washing in the solutions of nitric (specimen #1-C), sulfuric (specimen #2-C) and hydrochloric (specimen #3-C) acids; (3) annealing of the washed specimens #1-C, #2-C, and #3-C at 823 K for 30 min (specimens #1-CT, #2-CT, #3-CT); and (4) annealing of the specimens at 823 K for 30 min with the subsequent washing in a hydrochloric acid solution (specimens #1-TC, #2-TC, and #3-TC). To reveal the influence of the thermochemical treatment at each stage, the phase composition was studied by the X-ray diffraction spectroscopy (XRD) with an X-ray diffractometer DRON4-07 (Co-radiation) and the X-ray phase analysis (JSM-840 microscope). Elemental composition was determined by the X-ray microprobe analysis relative to the composition

of a gold film deposited on the surface of the specimen (three  $500 \times 500 \mu\text{m}^2$  areas were selected in each case). Besides, the temperature dependencies of the magnetic susceptibility were measured within the temperature range of 300–850 K using a standard Faraday technique [19] upon heating and cooling of the specimens. The heating and cooling rates did not exceed 10 K/min.

## Results and Discussion

Figures 1–3 display X-ray diffraction patterns obtained at different stages of the thermochemical treatment for a series of NCM specimens: Fig. 1—specimen #1, Fig. 2—specimen #2, Fig. 3—specimen #3. Figures 4–6 show

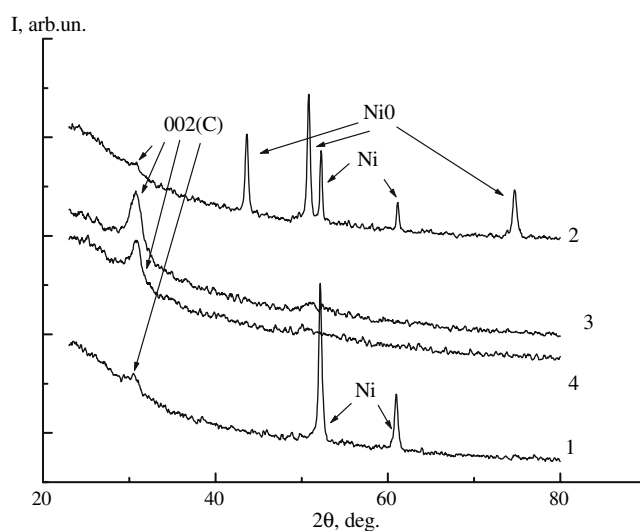


**Fig. 1** XRD patterns for a series #1 of NCM: 1, as-prepared NCM sample; 2, #1-T; 3, #1-CT; 4, #1-TC

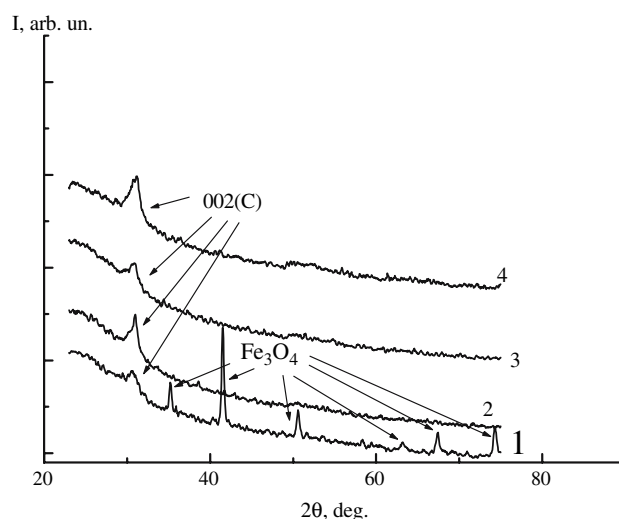


**Fig. 2** XRD patterns for a series #2 of NCM: 1, as-prepared NCM sample; 2, #2-C; 3, #2-CT; 4, #2-TC

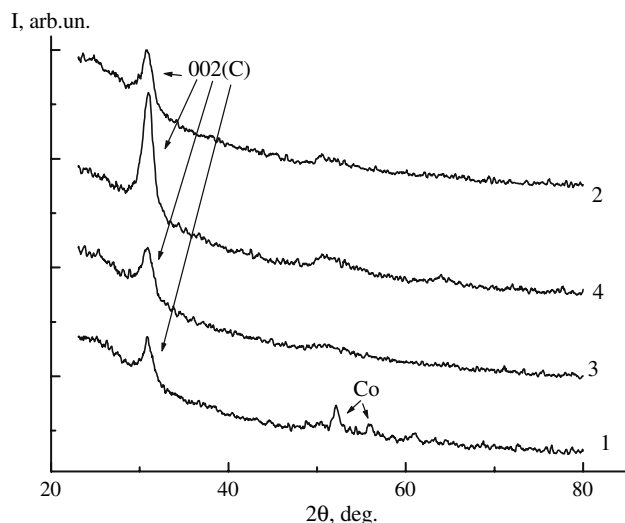


**Fig. 3** XRD patterns for a series #3 of NCM: 1, as-prepared NCM sample; 2, #3-C; 3, #3-CT; 4, #3-TC

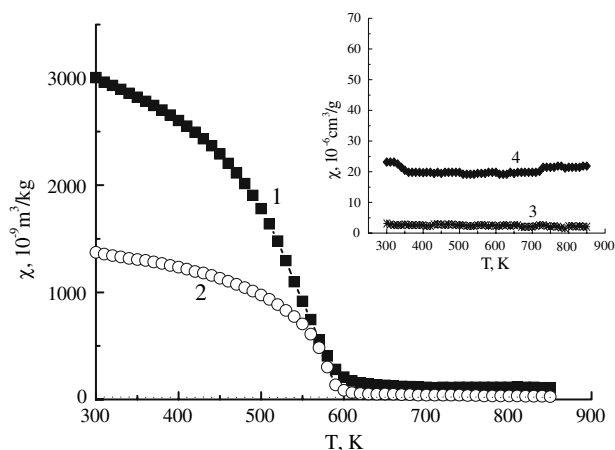


**Fig. 4**  $\chi(T)$  dependency for specimens #1 after different stages of thermochemical treatment: 1, #1 (source); 2, #1-T; inset: 3, #1-CT; 4, #1-TC

temperature dependencies of the magnetic susceptibility for the same specimens.

One can notice that the character of the XRD spectra for each NCM specimen is substantially modified in the process of thermochemical treatment. The low intensity (002) reflections of graphite and distinct reflections of the catalyst are observed for all the source specimens. As a result of the thermochemical treatment the ratio of the intensities of graphite and catalysts reflections changes: the intensity of the graphite peak increases, while those for the catalysts decrease and eventually disappear. Such behavior reflects the changes in the content of these phase constituents. A thorough analysis of the XRD data for the compositional variation of different carbon phases is presented in Ref. [20].

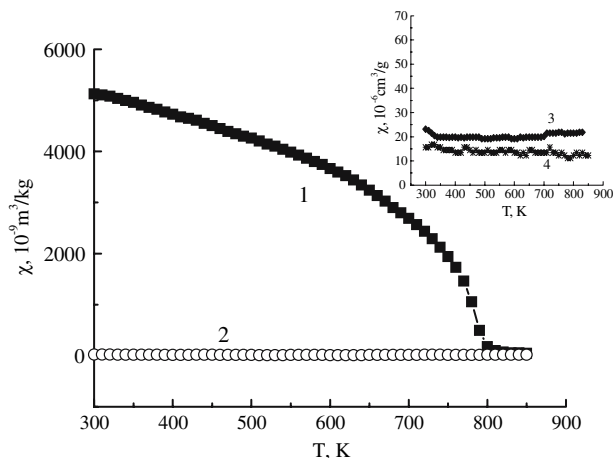


**Fig. 5**  $\chi(T)$  dependency for specimens #2 after different stages of thermochemical treatment: 1, #2 (source); 2, #2-C; inset: 3, #2-CT; 4, #2-TC

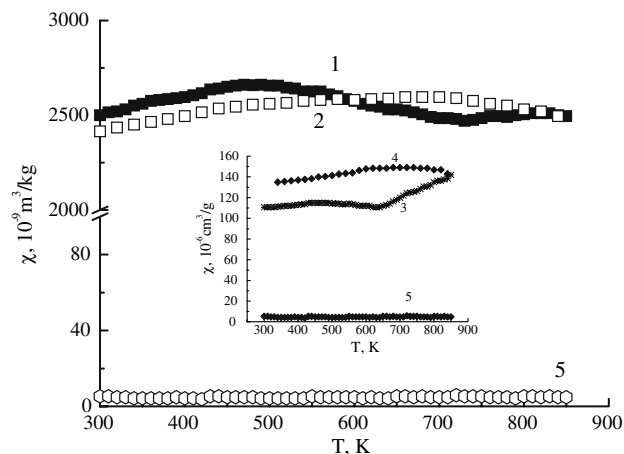


**Fig. 6**  $\chi(T)$  dependency for specimens #3 after different stages of thermochemical treatment: 1 and 2, #3 (heating and cooling, respectively); 5, #3-TC; inset: 3 and 4, #3-C (heating and cooling, respectively); 5, #3-TC

Let us consider the variation of the catalyst content. The as-prepared specimens under study exhibit a ferromagnetic behavior due to the presence of ferromagnetic catalysts, namely, nickel, cobalt, and iron oxide,  $\text{Fe}_3\text{O}_4$ , in the specimens #1, #3, and #2, respectively.

As it was stated earlier, the sharp intense reflections of Ni are observed in the XRD pattern for specimen #1. The data of the X-ray microprobe analysis (see Table 1) also indicates a significant content (>60%) of Ni. The character of the magnetic susceptibility  $\chi(T)$  curve for the source material is typical for NCM containing a substantial amount of nickel. However, estimates of the Curie temperature employing approximation of the magnetization with a zero value (see Refs. [21, 22] for details) have

**Table 1** The content of elements in the source and thermochemically treated specimens of #1, #2, #3 series

Element	Content (%) <sup>a</sup>					
	#4	#4-CT	#5	#5-TC	#6	#6-TC
Ni	60	<1	<1	0	<1	0
Fe	0	0	40	1.5	<1	0
Co	<1	0	0	0	16	<1

<sup>a</sup> Error in determining the elemental composition is 0.5%

shown that a distinct characteristic of this specimen was a lower value of the Curie point (ca. 590 K) compared to that of a bulk nickel (631 K) [21]. From the analysis of a thermomagnetic behavior of carbon-metal nanocomposites performed in earlier studies [19, 22], this particular feature is thought to be directly associated with the size of nickel particles ( $L$ ) and indicates their high dispersity. The results reported in Ref. [19, 22] demonstrated a good agreement between the calculated and the experimental values of the particle size. According to Ref. [22], the relationship between the Curie temperature  $T_C$  and  $L$  could be expressed as:

$$L = 3d \left[ \frac{T_C}{2(T_{Cb} - T_C)} - 1 \right], \quad (1)$$

where  $d$  is the atomic diameter,  $T_{Cb}$  is the Curie temperature for a bulk nickel.

Estimation of the size of nickel particles in the source NCM #1 using Eq. 1 gives  $L \sim 5$  nm. The character of the  $\chi(T)$  curve after annealing does not change, however, the absolute value of the room temperature susceptibility decreases by a factor of two. This may be from the oxidation of nickel particles upon heat treatment in air and the formation of the antiferromagnetic NiO phase. Indeed, the XRD data (Fig. 1, curve 2) indicate presence of both of nickel oxide and pure nickel at this stage of the thermochemical treatment. At the same time, the increase of  $T_C$  up to 612 K could be considered as a result of nickel re-crystallization. The value of  $L$  increases up to about 12 nm. The intensities of Ni and NiO reflections decrease almost to zero for specimen #1 after subsequent stages of the thermochemical treatment (Fig. 1, curves 3 and 4). This indicates either a total removal of the catalyst or a disintegration of the nickel particles. In any case, it is impossible to estimate the content of the metallic ferromagnetic component from the XRD data, although, according to the X-ray microprobe analysis data, the Ni content is about 1% (Table 1). For specimen #1-CT, as well as for #1-TC, a sharp decrease of  $\chi$ -values was observed. Here, the magnetic susceptibility remains almost invariable within the whole temperature range indicating absence of ferromagnetic phases. However, the values of  $\chi$

for these two specimens were found to be substantially higher than for the carbon support suggesting presence of antiferromagnetic or, perhaps, superparamagnetic metal-containing phases. At the same time, the value of  $\chi$  for specimen #1-TC is somewhat higher compared to that of specimen #1-CT, i.e. formation of a NiO layer on the surface of Ni particles upon the thermal treatment reduces the efficiency of acidic chemical treatments.

XRD data (Fig. 2) revealed presence of  $Fe_3O_4$  in the NCM specimens, which were obtained using the iron oxide catalyst. Analysis of the  $\chi(T)$  dependencies (Fig. 5) and the value of the Curie temperature for specimen #2 also allow to conclude that the catalyst particles present in this NCM in the form of  $Fe_3O_4$  iron oxide. The value of the Curie temperature determined from the  $\chi(T)$  dependency is 800 K, which is 58 K lower than the Curie temperature for a bulk  $Fe_3O_4$  (858 K) [21]. Estimation of the particle size according to Eq. 1 gives the value of about 15 nm. The thermochemical treatment (either initially a chemical treatment followed by a heat treatment of the source material or vice versa) substantially reduces the relative amount of the magnetic phase in the NCM. As in the case of the Ni catalyst, this is confirmed by the data of the X-ray phase analysis (Fig. 2) and X-ray microprobe analysis (Table 1). The susceptibility of these specimens decreases and becomes almost temperature-independent. Results for  $\chi(T)$  revealed the presence of the refuses of the metal-containing phases. On the other hand, any sequence of stages of the thermochemical treatment (specimens #2-CT and #2-TC) results in almost the same reduction of the  $\chi$ -values. Thus, regardless of the sequence of those stages, the composition of the catalyst refuses in this NCM turns out to be almost the same.

Figure 6 illustrates the temperature dependencies of  $\chi$  for specimens #3 (cobalt catalyst). The XRD analysis reveals the presence of Co particles for this specimen (Fig. 3, curve 1). As it can be seen from Fig. 6, a complex temperature behavior of  $\chi$  is observed for the source specimen. The observed specific behavior of the  $\chi(T)$  curves is thought to be caused by phase transformations of cobalt upon heating (in particular, by its partial oxidizing). The X-ray studies do not reveal presence of Co or cobalt oxides at any subsequent stages of the thermochemical treatment. This could be caused by a high dispersity of Co or cobalt oxide particles. However, the thermomagnetic studies allow qualitative analysis of the transformations in the ferromagnetic phases resulting from the thermochemical treatment. Washing of the source specimen in a hydrochloric acid solution (#3-C) leads to a substantial (more than tenfold) reduction of  $\chi$ . However, no significant changes in the character of the  $\chi(T)$  curve were observed. This observation suggests that such the thermochemical treatment procedure does not in general allow a complete

removal of the catalyst refuses. A different situation is observed at further stages of the thermochemical treatment. Annealing of the source NCM specimen and the subsequent washing in a hydrochloric acid solution (#3-TC) results in a sharp decrease (more than by two orders) of the  $\chi$ -values. Moreover, the magnetic susceptibility is almost independent of temperature. This indicates an extremely low content of the metal catalyst in specimen #3-TC. Thus, the proposed scheme of NCM cleaning from cobalt catalyst refuses is quite efficient. This conclusion is in agreement with the data of the X-ray microprobe analysis (see Table 1).

## Conclusions

We performed studies of the temperature dependence of the magnetic susceptibility of CNT-containing NCM specimens synthesized using different transition metal (Fe, Co, Ni) oxides as catalysts. Our results demonstrated that magnetometry is an effective tool to control the content of ferromagnetic constituents. This method is capable to detect even low contents of metal catalyst. The proposed thermochemical treatment protocols result in effective cleaning of the source NCM from the refuses of ferromagnetic phases. The efficiency of cleaning is determined by the sequence of thermochemical treatment steps as well as the type of the catalyst.

**Acknowledgments** This work was supported by the CRDF Grant (UKP1-2616-KV-04). The authors acknowledge Dr. E. V. Prylutsky who provided the NCM specimens.

## References

1. A.V. Eletskiy, Usp. Fiz. Nauk (in Russian) **172**, 401 (2002)
2. S. Arepalli, J. Nanosci. Nanotechnol. **4**, 317 (2004)

3. H. Dai, A. Rinzler, P. Nikolaev, A. Thess, D. Colbert, R.E. Smalley, Chem. Phys. Lett. **260**, 471 (1996)
4. R. Andrews, D. Jacques, D. Qian, T. Rantell, Acc. Chem. Res. **35**, 1008 (2002)
5. C.T. Kingston, B. Simard, Anal. Lett. **36**, 3119 (2003)
6. H. Dai, Acc. Chem. Res. **35**, 1035 (2002)
7. K. Awasthi, A. Strivastava, O.N. Strivastava, J. Nanosci. Nanotechnol. **5**, 1616 (2005)
8. J.E. Herrera, L. Balzano, F. Pompeo, D.E. Resasco, J. Nanosci. Nanotechnol. **3**, 1 (2003)
9. M. Monthieux, B.W. Smith, B. Bouteaux, A. Claye, J.E. Fischer, D.E. Luzzi, Carbon **39**, 1251 (2001)
10. A. Moisala, A.G. Nasibulin, E.I. Kaupponen, J. Phys.: Condens. Matter **15**, S3011 (2003)
11. K. Kuwana, H. Endo, K. Saito, D. Qian, R. Andrews, E.A. Grulke, Carbon **43**, 253 (2005)
12. M.S. Dresselhaus, G. Dresselhaus, A. Jorio, A.G. Souza Filho, R. Saito, Carbon **40**, 2043 (2002)
13. S.V. Terekhov, E.D. Obratsova, *Laser heating method for estimation of carbon nanotube purity*, in Abstracts and Programme EUROCARBON 2000. 1st World Conf. on Carbon, vol. 1 (Berlin, 2000), p. 465
14. A.S. Lobach, N.G. Spitsina, S.V. Terekhov, E.D. Obratsova, Fiz. Tverd. Tela (in Russian) **44**, 457 (2002)
15. H.M. Cheng, F. Li, X. Sun, S.D.M. Brown, M.A. Pimenta, A. Marucci, G. Dresselhaus, M.S. Dresselhaus, Chem. Phys. Lett. **289**, 602 (1998)
16. O. Prilutskiy, E.A. Katz, A.I. Shames, D. Mogilevsky, E. Mogilko, E. Prilutskiy, S.N. Dub, Fuller. Nanotubes Carbon Nanostruct. **13**, 53 (2005)
17. L.Yu. Matzui, Yu.I. Prylutskiy, I.V. Ovsienko, T.A. Len, P. Scharff, Fuller. Nanotubes Carbon Nanostruct. **13**, 259 (2005)
18. M. Monthieux, B.W. Smith, B. Bouteaux, Carbon **39**, 1251 (2001)
19. L. Matzui, M. Babich, M. Zakharenko, L. Nakonechna, Mater. Sci. Forum **373–376**, 241 (2000)
20. I.V. Ovsienko, T.A. Len, L.Yu. Matzui, O.A. Golub, Yu.I. Prylutskiy, P. Eklund, Mater. Sci. Eng. C **26**, 1180 (2006)
21. S.V. Vonsovskiy, Magnetism (Nauka Moscow, 1971, in Russian)
22. M.G. Babich, T.A. Len, L.Yu. Matzui, M.P. Semenko, L.L. Vovchenko, M.I. Zakharenko, *Magnetic properties of nanostructured Ni deposited on graphite supporter*, in Proceeding of International School-Seminar “New magnetic materials of microelectronics” (Moscow, 2002) (in Russian), p. 886